Proceedings of the IASS 2024 Symposium
Redefining the Art of Structural Design
August 26-30, 2024, Zurich Switzerland
Philippe Block, Giulia Boller, Catherine DeWolf,
Jacqueline Pauli, Walter Kaufmann (eds.)

Numerical Investigation of 3D-printed Spinal Braces

Iason ROSSETOS, Stefanos VOULGARIS, George KAZAKIS, Charis J. GANTES* and Nikos D. LAGAROS

* School of Civil Engineering, National Technical University of Athens
9 Heroon Polytechniou St., Zografou, 15780 Athens, Greece
chgantes@central.ntua.gr

Abstract

Spinal braces are shell-type structures used by patients exhibiting deformities of the spine, relying on basic engineering principles, such as three-point bending and inversion forces. The aim of the present study is to describe the finite element simulation of a spinal brace, as part of a methodology to achieve 3D printed, lightweight, personalized braces for comfortable use by patients. The applied loads simulate the tightening of the straps on the rear faces of the brace, while the support pad regions represent the main contact areas between brace and body, where the corrective forces develop. To facilitate convergence of the optimization algorithm, boundary conditions were established by employing elastic springs at the support pad areas that simulate the interaction between brace and human skin, rather than using nonlinear contact-type elements. The mechanical properties of polylactic acid, which has been selected as the brace material, were obtained through experimental tests of 3D printed specimens. The developing stress field and deformation of the brace, as well as spring forces representing the pressure exerted on the patient's body by the brace, are illustrated to describe the structural response. In addition, initial results of a simple Topology Optimization simulation are briefly presented.

Keywords: spinal brace, nonlinear finite element analysis, topology optimization, 3D printing.

1. Introduction

Idiopathic scoliosis (IS) is a three-dimensional spinal deformity that affects millions of people, especially teenagers and adolescents, as described by Chan et al. [1]. The non-surgery way to treat it is by using a spinal brace to limit the Cobb angle progression, described by Negrini et al. [2], Kuroki [3] and Ali et al. [4]. At present, the predominant scoliosis braces in clinical practice are the Boston Brace and the Milwaukee Brace [5-7], both of which are frequently cited as cumbersome and inadequately comfortable for patients, as reported by Zarea et al. [5], Olafsson et al.[6] and Khan et al. [7] . Towards optimizing spine brace design to achieve comfortable use by patients, a research project is ongoing to develop a procedure comprising scanning of the patient's body, advanced numerical modeling, topology optimization and additive manufacturing, to design and 3D print lightweight, personalized braces, to be verified by experimental testing followed by clinical trials. In the present paper the early stages of numerical modeling and topology optimization of this effort are reported. Similar studies have been reported in the literature like Aubin et al. [8], Ronca et al. [9], Redaelli et al. [10] and Rossetos et al. [11], focusing on simulating the structural behavior of a spinal brace with the finite element method.

In the present study, the Abaqus CAE v. 2021 software [12] is employed and CAD scans (Meshmixer v. 3.5.474 by Autodesk [13]) of an actual spinal brace are utilized for the numerical simulation. The use of laser scanning technology enables the acquisition of highly detailed anatomical data in a noninvasive manner, allowing for tailoring product designs in medical applications, Kim et al. [14] and Taneva et al. [15]. Regarding the mechanical characteristics of brace materials, researchers have commonly relied on

the properties of polypropylene and polyethylene, as presented by Grycuk et al. [16] and Mafi et al.[17], which have historically constituted the primary materials for spinal braces.

In recent years several researchers have proposed procedures integrating advanced design methods and additive manufacturing for the realization of lightweight, easy to use personalized braces. In a recent comparative study, Ronca et al. [9] evaluated the suitability of four different materials for 3D printed spinal braces. Redaelli et al. [10] presented the advantages and disadvantages of 3D printed spinal braces in comparison to the traditional ones. Rossetos et al. [11] presented a simulation utilizing the mechanical properties of PLA (Polylactic Acid), obtained from laboratory testing, to assess the structural response of 3D-printed spinal braces.

A critical aspect of numerical modeling is the incorporation of loads and boundary conditions. In publications by Chan et. al [1], Grycuk et. al [16] and [18]- [24] experimental tests were employed to elucidate a realistic range of values of the loads, pressures and corrective forces between the human body and the spinal brace. For simulation purposes, a main loading scenario refers to the case of strap tensioning causing corrective forces to the human body.

Regarding boundary conditions, various simplified approaches employing pinned or fixed supports have been explored in previous research [16,17]. In addition, compelling evidence regarding the interaction between the human body and spinal braces is provided in Rossetos et. al [11], Liao et. al [20], Ali et. al [24] and Perie et. al [25], elucidating the generation of pressures but also delving into more intricate simulations of contact between brace and human body, which require nonlinear analysis. The present research endeavors to simulate this interaction with spring elements, to facilitate convergence of the optimization algorithms. To achieve this objective, it is imperative to consider the stiffness properties of the human body to estimate a realistic range of the spring stiffness. In Cua et. al [26], Griffin et. al [27], Graham et. al [28], Wei et. al [29] and Zhang et. al [30] comprehensive insights into the stiffness properties and friction of the human body and skin are offered, accompanied by experimental findings on skin displacement under varying pressures. Notably, these studies reveal that the stiffness of the human skin exhibits regional variations, with observed displacements ranging from 0 to 70 mm under applied pressures of 200 mbar (20 kPa) as described by Cua et. al [26].

Considering the creation of lightweight spinal braces, some attempts have been made, most notably by Liao et al. [31] and Zhang and Kwok [32]. Liao et al. performed Topology Optimization on a Boston brace using a heat image mapping of the pressures as loading conditions and the trap areas as boundaries. Zhang & Kwok presented different implementations of Topology Optimization on casts and braces.

2. Numerical Modeling

The different steps of the numerical modeling and analysis methodology are described in the present section.

2.1. Laser scanning procedure and file preparation.

The process of laser scanning the human torso utilizes advanced three-dimensional imaging technologies, transforming the upper body segment, covering the chest to the spine, into a detailed digital model. To achieve this, the following steps are undertaken. a) Pre-scan preparations including dress of patients in fitted, non-reflective apparel. b) Equipment calibration to the manufacturer's specifications to ensure high precision in measurements. c) Patient positioning within a specified zone for scanning. d) Execution of laser scanning, during which laser beams are projected onto the patient's torso, recording distance measurements from a multitude of points across the surface and generating a 'point cloud', in which data from varied angles are used to craft a detailed 3D model of the torso, often in several scanning rounds. e) Integration of scanning data to form a unified and accurate three-dimensional representation, involving alignment of individual point clouds. f) Mesh creation from point clouds, made up of interconnected triangular elements.

Following the creation of the torso model, the next step involves preparing the model for spinal brace design using the CAD software Meshmixer by AutoDesk [13]. One significant hurdle in this phase is the management of sudden geometric variations within the scan, which might hinder the brace modeling

efforts. These imperfections, particularly around the brace edges, are smoothed out to create a more uniform domain. Finally, to facilitate the utilization of shell finite elements in the modeling process, the thickness of the original scan is removed and the model is exported to an stl formatted file.

2.2. Geometry and numerical model

After the scanning procedure, the STL file is imported into Abaqus CAE software environment. The shape and indicative dimensions of the examined spinal brace are presented in Figure 1.

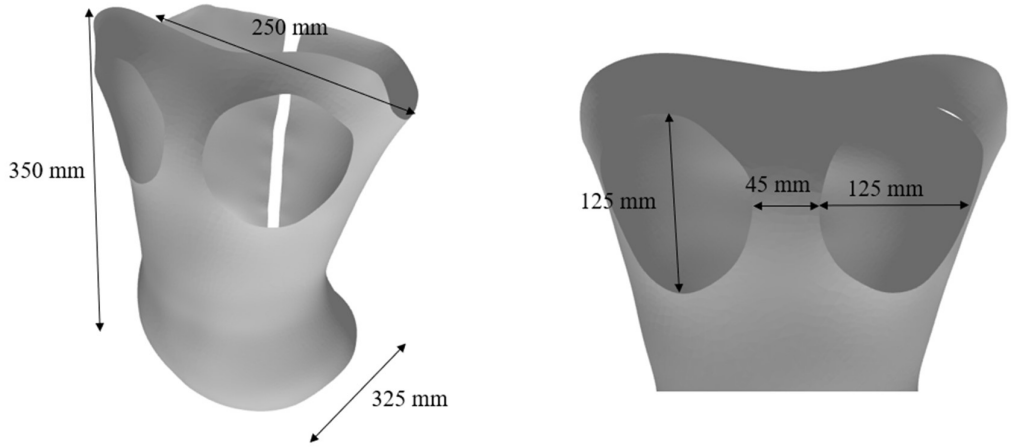

Figure 1 : Dimensions of spinal brace

A numerical model of the spinal brace utilizing shell finite elements has been developed, with a cross-sectional thickness assigned at 4 mm. Given the intricate geometry of the brace, characterized by numerous curves and lack of symmetry, discrete surfaces have been delineated to enhance clarity and accuracy in applying loads and boundary conditions. To this end, the brace has been partitioned along planes parallel to the three principal axes, as in Figure 2a,b. A free meshing with triangular elements, presented in Figure 2c, is assigned due to the curved surface of the brace. It constitutes an unstructured mesh, as implied by its designation, rendering it adaptable to various geometric configurations. The average surface area of each triangular element is estimated to be approximately 10.3 mm².

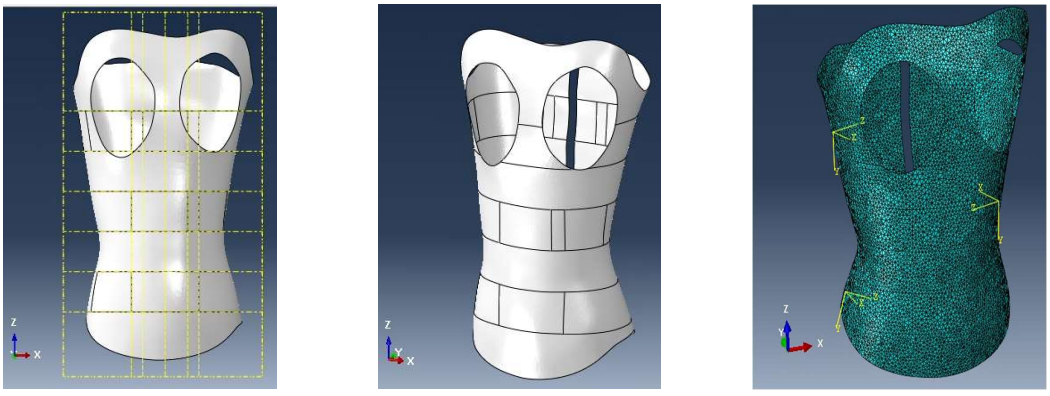

(a) (b) (c)

Figure 2 : Spinal brace: a) Regions defined by parallel planes, b) 3D view, c) Free meshing

2.3. Material

Conventional spinal braces are made of polypropylene and polyethylene, adopted also in simulations by Grycuk et. al [16] and Mafi et. al [17]. The objective of this study, however, is to assess the structural performance of a 3D printed spinal braces, therefore, material properties of Polylactic Acid (PLA) are designated for the brace. In prior research by Rossetos et. [11], the material properties of anisotropic PLA were determined through laboratory tensile testing, as detailed in Table 1.

Table 1: Material properties of 3D printed PLA simulation

Material	E_1	E_2	v_{12}	G_{12}	G_{13}	G_{23}
	MPa	MPa		MPa	MPa	MPa
PLA	3045	2898	0.33	987	1012	987

The tensile strength of PLA in directions 1 and 2 was found to be approximately 49 MPa and 35 MPa, respectively.

2.4. Load and boundary conditions.

A primary loading scenario, predicated on the application of strap tension at the rear side of the brace, has been simulated, considered important for the generation of corrective forces exerted upon the human body. This scenario is based on the concept of three-point bending and inversion forces, aiming to restrict the progression of spinal inclination. Specifically, on the rear face of the brace, designated surfaces, as presented in Figure 3a, are subjected to strap tensions of 10 N, within the range reported by Ali et. al [22]. Consequently, corrective forces emerge at the surfaces of supporting pads with dimensions of 50 mm x 50 mm (Figure 3b), due to the prescribed boundary conditions applied in these areas.

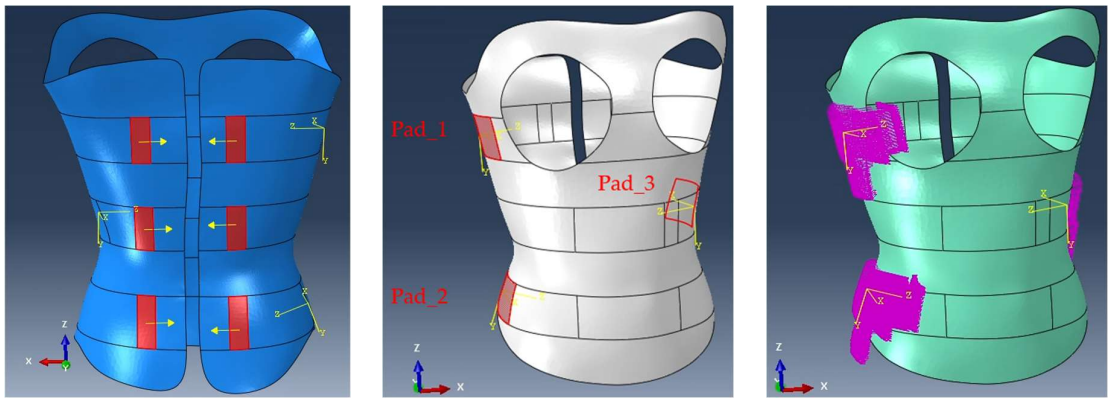

(a) (b) (c)

Figure 3: a) Strap surfaces and concentrated forces, b) Supporting pad surfaces, c) Supporting pad springs

The assignment of boundary conditions is a critical aspect of spinal brace simulations. Grycuk et. al [16] and Mafi et. al [17], adopt simplified approaches to boundary conditions, often employing pinned or fixed supports at specific parts of the brace. However, these approaches neglect the deformability of the body, and tend to overestimate the pressures exerted on the body from contact with the brace. In the present study, spring elements are employed to characterize the behavior and response of human skin upon contact with the brace. From research by Cua et. al [26], it is noted that under a 200 mbar pressure, the displacement of a 3mm² test area is 0.68 mm. Taking this into consideration, the bedding stiffness transversely to the plane of the pads is calculated as:

$$K_{z,spring} = \frac{0.02}{0.68}\frac{\frac{\mathrm{N}}{\mathrm{mm}^2}}{\mathrm{mm}} = 0.029\,\frac{\mathrm{N}}{\mathrm{mm}^3} \tag{1}$$

Reducing to the surface area of each triangular finite element of the numerical model, which is equal to 10.3 mm² at an average, the stiffness of a representative transverse spring is obtained:

$$k_{z,spring} = 0.029\,\frac{\mathrm{N}}{\mathrm{mm}^3}\ \mathrm{x}\ 10.3\ \mathrm{mm}^2 = 0.3\,\frac{\mathrm{N}}{\mathrm{mm}} \tag{2}$$

In order to describe the friction between brace and human body, spring elements are also assigned in the tangential directions x and y, with stiffness equal to 40% of the transverse one:

$$k_{x,y,spring} = 0.4\ \mathrm{x}\ k_{z,spring} = 0.4\ \mathrm{x}\ 0.3\,\frac{\mathrm{N}}{\mathrm{mm}} = 0.12\,\frac{\mathrm{N}}{\mathrm{mm}} \tag{3}$$

One transverse and two tangential spring elements are allocated to each node within the supporting pad area, as presented in Figure 3c.

3. Analysis Results

Linear static analyses have been conducted, using the geometry, applied loads, and boundary conditions outlined in the preceding section. The analysis results are presented in this section pertaining to the induced stresses and deformations of the brace and the developing pressures between the brace and the patient's body.

3.1. Stresses and displacements of the brace

The induced von Mises stresses describing the overall stress condition of the spinal brace are presented in Figure 4a for the front face of the brace, and in Figure 4b for the rear face. The maximum stresses are in the order of 2.9 MPa, much lower than the tensile strength of PLA in both directions. The resulting displacements of the spinal brace in the three directions are depicted in Figure 5. The maximum displacements are in the order of 5.68mm and 4.55mm in the two horizontal directions and 0.66mm in the vertical direction and are observed near the straps.

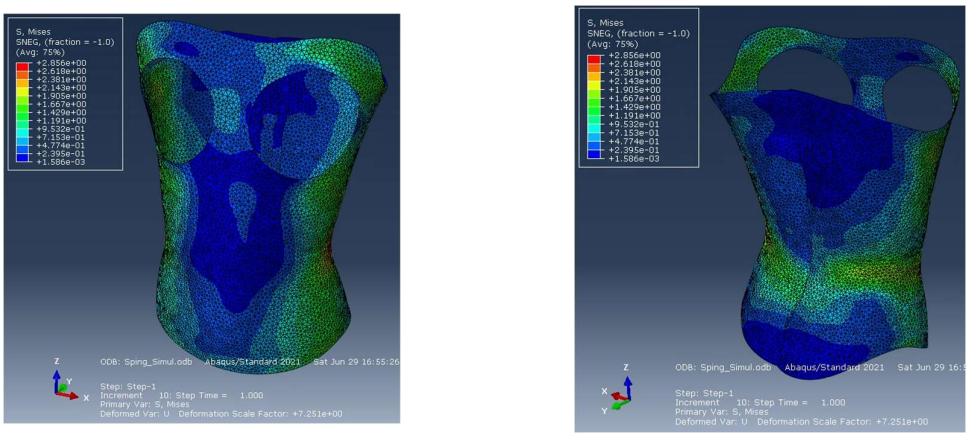

(a) (b)

Figure 4: Von Mises stresses in MPa at: a) the front face of the brace, b) the rear face of the brace

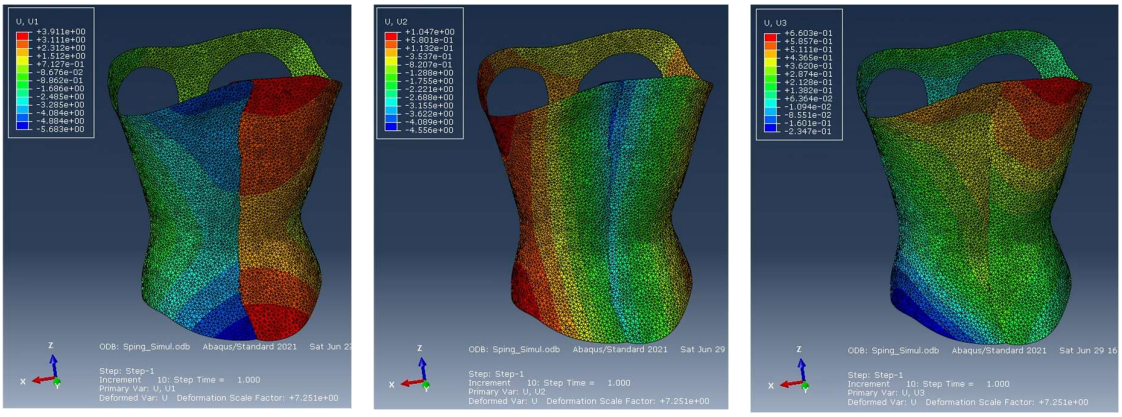

(a) (b) (c)

Figure 5: Displacements of the spinal brace in the global coordinate system in mm: a) X axis, b) Y axis, c) Z axis

3.2. Pressures between the brace and the body

The developing pressures between the supporting pads and the patient's body regions are obtained from the forces of the springs. This is an important response parameter, facilitating an assessment of the safety

and comfort of the brace design. All spring forces and corresponding displacements at each pad, are illustrated in the subsequent Figure 6. It is observed that the pressures and displacements at pad 3, which is on one side of the brace, are approximately higher than the ones in pads 2 and 3, which are both on the other side. By dividing the maximum spring force by the average area of the triangular finite element, which is equal to 10.3 mm^2, we obtain an estimate of the maximum pressure exerted on the human body at each pad. The results are presented in Table 2.

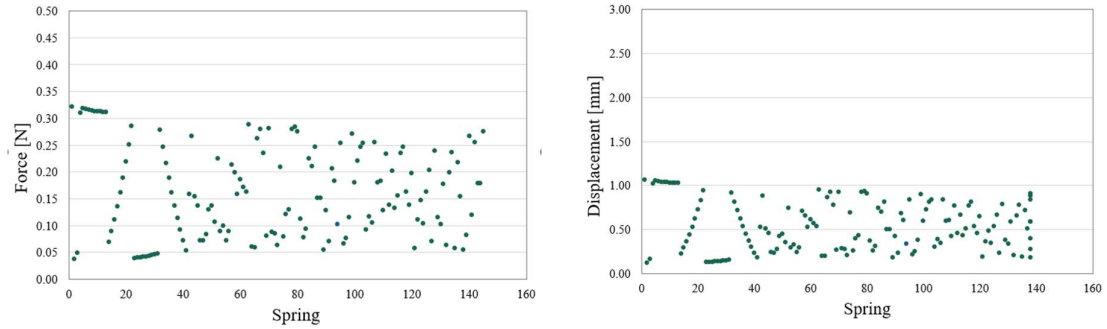

Supporting pad 1

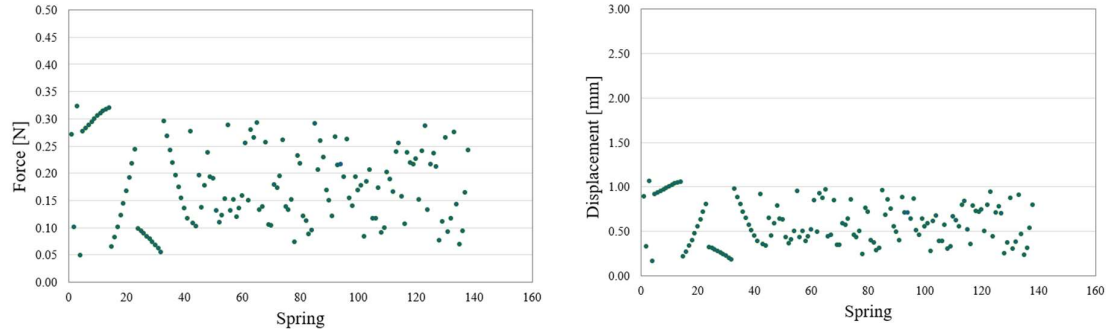

Supporting pad 2

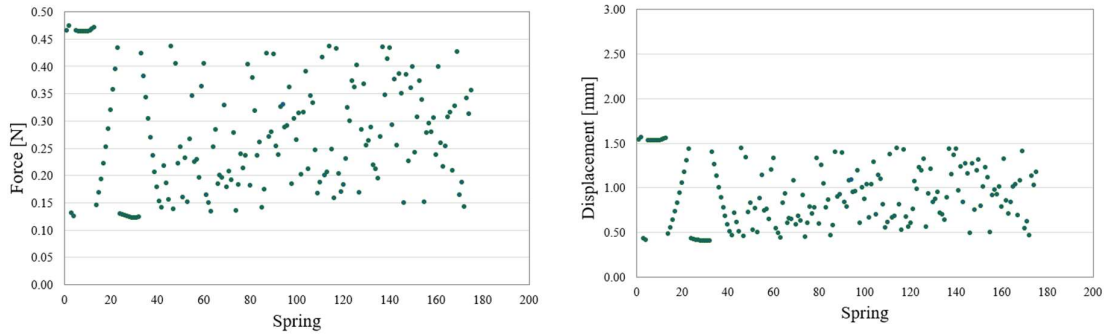

Supporting pad 3

Figure 6: Spring forces and relative displacements

Table 2: Maximum response quantities for each supporting pad

	Pad 1	Pad 2	Pad 3
Max force (N)	0.32	0.32	0.47
Max pressure (kPa)	31.23	31.35	46.09
Max displacement (mm)	1.06	1.07	1.57

Pham et. al [18], Ali et. al [22] and Loukos et. al [23] present a correlation between strap-elastic bands tension and resultant pressures, ultimately asserting that tension forces up to 20 N applied to the straps yield pressures ranging up to 10 kPa. Based on our numerical results, applying a tension of 10 N to the straps led to the generation of pressures in the order of 46kPa, as a maximum value which exceeds the acceptable range delineated in the literature, suggesting a local incompatibility with human physiological safety standards. This is attributed to the unfavorable assumption adopted in this simulation, that the brace makes contact with the human body only over the areas of the three pads. The next step of our research will involve a more complex approach, where the brace is in contact with the entire body, which is expected to lead to a distribution of stresses over a wider area, thus alleviating the local stress maxima.

3.3 Topology Optimization

In this section initial results of the Topology Optimization procedure aiming at producing a lightweight spinal brace with a more attractive design are briefly presented. In this simulation the objective was to obtain a lightweight spinal brace, with similar response to the original brace model presented above. The results are illustrated in Figure 7. The full-scale Topology Optimization formulation of the spinal brace model is under development and a more detailed presentation of the procedure and its results will be presented in future work.

(a) (b)

Figure 7: Initial results of topologically optimized spinal brace a) rear face b) front face

4. Conclusion

Nonlinear finite element simulation of a spinal brace has been described in the present study, as part of a methodology to achieve 3D printed, lightweight, personalized spinal braces for comfortable use by patients and optimum effectiveness. The main aspects of brace operation, namely three-point bending, inversion forces and the inclusion of supporting pads, have been incorporated in the model, and tightening of the brace's straps has been simulated, aiming at acquiring a comprehensive understanding of the structural behavior. The interaction between the brace and the patient's body has been represented by transverse and tangential springs with realistic stiffness properties.

The obtained von Mises stresses across the entire brace do not exceed 3 MPa, which is considerably lower than the strength of the assumed PLA material and in accordance with the results reported in the literature. The obtained forces of spring elements applied to the nodes of the supporting pads provides insights into the interaction between the body and the brace. Namely, the pressure in pads 1 and 2 on one side of the brace is in the order of 31kPa, while in pad 3 on the opposite side around 46 kPa. These values locally exceed the pressures that can be tolerated by the human body, reported in the literature, which will be addressed in the next stage of this work, by allowing contact between the brace and the human body over wider areas.

The creation of lightweight and more appealing spinal braces can be achieved by implementing optimization procedures on the spinal brace model. Towards that goal, initial Topology Optimization

results have been presented. A further investigation of the parameters for implementing this formulation is being conducted. In the case of spinal braces, the classical Topology Optimization formulation seems appealing, due to the low stress field compared to the material's strength. Considering the classic approach, parameters as the target final volume as well as additional constraints will be considered and their effect on the final design will be evaluated.

Acknowledgements

This research was supported by the OrThoP3Dics project: "Topology optimization of 3D printed patient-specific spinal braces" (No.: TAEDK-06191) belonging to the National Recovery and Resilience Plan, Greece 2.0 Project.

References

[1] W. Y. Chan, J. Yip, K.-L. Yick, S.-P. Ng, L. Lu, K. M.-C. Cheung, K. Y.-H. Kwan, J. P.-Y. Cheung, K. W.-K. Yeung, and C.-Y. Tse, "Mechanical and Clinical Evaluation of a Shape Memory Alloy and Conventional Struts in a Flexible Scoliotic Brace," Annals of Biomedical Engineering, vol. 46, pp. 1194-1205, August 2018.

[2] S. Negrini, A. Aulisa, P. Cerny, J. de Mauroy, J. McAviney, A. Mills, et al., "The classification of scoliosis braces developed by SOSORT with SRS, ISPO, and POSNA and approved by ESPRM," European Spine Journal, vol. 31, pp. 980-989, February 2022

[3] H. Kuroki, "Brace treatment for adolescent idiopathic scoliosis," Journal of Clinical Medicine, vol. 7, p. 136, April 2018.

[4] A. Ali, V. Fontanari, M. Fontana, and W. Schmolz, "Spinal Deformities and Advancement in Corrective Orthoses," Bioengineering, vol. 8, no. 2, December 2020.

[5] M. Zarea, G. Aminian, M. Khosravi, and R. Baghaei, "Effect of Milwaukee Brace on Quality of Life in Adolescents with Idiopathic Scoliosis," Journal of Clinical Physiotherapy Research, vol. 5, p. e13, 2020.

[6] Y. Olafsson, H. Saraste, V. Söderlund, and M. Hoffsten, "Boston Brace in the Treatment of Idiopathic Scoliosis," Journal of Pediatric Orthopedics, vol. 15, p. 524, 1995.

[7] M. J. Khan, V. M. Srinivasan, and A. H. Jea, "The History of Bracing for Scoliosis," Clinical Pediatrics, vol. 55, pp. 320-325, 2015.

[8] C. Aubin, N. Cobetto, J. Clin, F. Desbiens-Blais, H. Labelle, S. Le May, and S. Parent, "Improved Brace Design Combining CAD/CAM And Finite Element Simulation For The Conservative Treatment Of Adolescent Idiopathic Scoliosis (AIS): Preliminary Results Of A Randomized Control Trial," in *Proceedings of the 10th Meeting of the International Research Society of Spinal Deformities (IRSSD 2014 Sapporo)*, Sapporo, Japan, 29 June-2 July 2014.

[9] A. Ronca, V. Abbate, D. F. Redaelli, F. Storm, G. Cesaro, C. De, A. Sorrentino, G. Colombo, F. Paolo, and L. A. Ambrosio, "Comparative Study for Material Selection in 3D Printing of Scoliosis Back Brace," Materials, vol. 15, p. 5724, August 2022.

[10] D. F. Redaelli, V. Abbate, F. A. Storm, A. Ronca, A. Sorrentino, C. De Capitani, E. Biffi, L. Ambrosio, G. Colombo, and P. Fraschini, "3D printing orthopedic scoliosis braces: A test comparing FDM with thermoforming," International Journal of Advanced Manufacturing Technology, vol. 111, pp. 1707-1720, October 2020.

[11] I. Rossetos, C.-J. Gantes, G. Kazakis, S. Voulgaris, D. Galanis, F. Pliarchopoulou, K. Soultanis, N. D. Lagaros, "Numerical Modeling and Nonlinear Finite Element Analysis of Conventional and 3D-Printed Spinal Braces," Applied Sciences, vol. 14, p. 1735, February 2024.

[12] Simulia Abaqus CAE. Available online: https://www.3ds.com/products/simulia/abaqus/cae (accessed on 24 January 2024).

[13] Meshmixer by Autodesk. Available online: https://meshmixer.com (accessed on 24 January 2024).

[14] J. Kim, G. Heo, and M. O. Lagravère, "Accuracy of laser-scanned models compared to plaster models and cone-beam computed tomography," The Angle Orthodontist, vol. 84, no. 3, pp. 443–450, Aug. 2013, doi: 10.2319/051213-365.1.

[15] E. Taneva, B. Kusnoto, and C. A. Evans, 3D Scanning, Imaging, and Printing in Orthodontics, IntechOpen, London, UK, 2015. Available online: https://www.intechopen.com/chapters/48165 (accessed on 24 January 2024).

[16] S. Grycuk and P. Mrozak, "Scoliosis Brace Finite Element Model and Preliminary Experimental Testing Using Electronic Speckle Pattern Interferometry," Applied Sciences, vol. 12, p. 3876, April 2022.

[17] M. Mafi, A. M. K. Niyaval, and S. Khanmohammadi, "Brace Simulation for Patients with Scoliosis: Biomechanical Comparison with Three Different Polymeric Materials," *BKK Medical Journal*, vol. 15, p. 161, June 2019.

[18] V.-M. Pham, A. Houilliez, A. Schill, A. Carpentier, B. Herbaux, and A. Thevenon, "Study of The Pressures Applied by A Cheneau Brace for Correction of Adolescent Idiopathic Scoliosis," *Prosthetics and Orthotics International*, vol. 32, pp. 345–355, July 2008.

[19] J. A. A. M. Van den Hout, L. W. Van Rhijn, R. J. H. Van den Munckhof, and A. Van Ooy, "Interface corrective force measurements in Boston brace treatment," *European Spine Journal*, vol. 11, pp. 332–335, December 2001.

[20] Y.-C. Liao, C.-K. Feng, M.-W. Tsai, C.-S. Chen, C.-K. Cheng, and Y.-C. Ou, "Shape Modification of the Boston Brace Using a Finite-Element Method with Topology Optimization," Spine, vol. 32, pp. 3014–3019, 2007.

[21] C.-L. Chung, D.-M. Kelly, J.-R. Steele, and D.-J. DiAngelo, "A mechanical analog thoracolumbar spine model for the evaluation of scoliosis bracing technology," *Journal of Rehabilitation and Assistive Technologies Engineering*, vol. 5, pp. 1–9, October 2018.

[22] A. Ali, V. Fontanari, W. Schmolz, and M. Fontana, "Actuator and Contact Force Modeling of an Active Soft Brace for Scoliosis," *Bioengineering*, vol. 9, p. 303, July 2022.

[23] I. Loukos, C. Zachariou, C. Nicopoulos, D. Korres, and N. Efstathopoulos, "Analysis of the corrective forces exerted by a dynamic derotation brace (DDB)," Prosthetics and Orthotics International, vol. 35, no. 4, pp. 365–372, July 2011.

[24] A. Ali, V. Fontanari, W. Schmolz, and S.-K. Agrawal, "Active Soft Brace for Scoliotic Spine: A Finite Element Study to Evaluate in-Brace Correction," *Robotics*, vol. 11, p. 37, March 2022.

[25] D. Périé, C. E. Aubin, M. Lacroix, Y. Lafon, and H. Labelle, "Biomechanical Modelling of Orthotic Treatment of the Scoliotic Spine Including a Detailed Representation of the Brace-Torso Interface," *Medical & Biological Engineering & Computing*, vol. 42, pp. 339–344, August 2003.

[26] A.-B. Cua, K.-P. Wilhelm, and H.-I. Maibach, "Elastic properties of human skin: Relation to age, sex, and anatomical region," *Archives of Dermatological Research*, vol. 282, pp. 283–288, October 1989.

[27] M.-F. Griffin, B.-C. Leung, Y. Premakumar, M. Szarko, and P.-E. Butler, "Comparison of the mechanical properties of different skin sites for auricular and nasal reconstruction," *Journal of Otolaryngology - Head and Neck Surgery*, vol. 46, p. 33, 2017.

[28] H.-K. Graham, J.-C. McConnell, G. Limbert, and M.-J. Sherratt, "How stiff is skin," *Experimental Dermatology*, vol. 28, suppl. 1, pp. 4–9, October 2018.

[29] J.-C.-J. Wei, G.-A. Edwards, D.-J. Martin, H. Huang, M.-L. Crichton, and M.-F. Kendall, "Allometric scaling of skin thickness, elasticity, viscoelasticity to mass for micro-medical device translation: from mice, rats, rabbits, pigs to humans," *Scientific Reports*, vol. 7, p. 15885, November 2017.

[30] M. Zhang and A.-F.-T. Mak, "In vivo friction properties of human skin," *Prosthetics and Orthotics International*, vol. 23, pp. 135-141, 1999.

[31] Liao, Y. C.; Feng, C. K.; Tsai, M. W.; Chen, C. S.; Cheng, C. K.; Ou, Y. C. Shape Modification of the Boston Brace Using a Finite-Element Method With Topology Optimization. Spine (Phila Pa 1976) 2007, 32 (26), 3014–3019. https://doi.org/10.1097/BRS.0b013e31815cda9c.

[32] Zhang, Y.; Kwok, T.-H. Customization and Topology Optimization of Compression Casts/Braces on Two-Manifold Surfaces. Computer-Aided Design 2019, 111, 113–122. https://doi.org/10.1016/j.cad.2019.02.005.